

Computing the dipole polarizability of ^{48}Ca with increased precision

M. Miorelli,^{1,2} S. Bacca,^{3,1,4} G. Hagen,^{5,6,*} and T. Papenbrock^{6,5}

¹*TRIUMF, 4004 Wesbrook Mall, Vancouver, British Columbia, V6T 2A3, Canada*

²*Department of Physics and Astronomy, University of British Columbia, Vancouver, British Columbia, V6T 1Z4, Canada*

³*Institut für Kernphysik and PRISMA Cluster of Excellence, Johannes Gutenberg-Universität Mainz, 55128 Mainz, Germany*

⁴*Department of Physics and Astronomy, University of Manitoba, Winnipeg, Manitoba, R3T 2N2, Canada*

⁵*Physics Division, Oak Ridge National Laboratory, Oak Ridge, Tennessee 37831, USA*

⁶*Department of Physics and Astronomy, University of Tennessee, Knoxville, Tennessee 37996, USA*

(Dated: July 2, 2018)

We compute the electric dipole polarizability of ^{48}Ca with an increased precision by including more correlations than in previous studies. Employing the coupled-cluster method we go beyond singles and doubles excitations and include leading-order three-particle-three-hole ($3p$ - $3h$) excitations for the ground state, excited states, and the similarity transformed operator. We study electromagnetic sum rules, such as the bremsstrahlung sum rule m_0 and the polarizability sum rule α_D using interactions from chiral effective field theory. To gauge the quality of our coupled-cluster approximations we perform several benchmarks with the effective interaction hyperspherical harmonics approach in ^4He and with self consistent Green's function in ^{16}O . We compute the dipole polarizability of ^{48}Ca employing the chiral interaction $\text{N}^2\text{LO}_{\text{sat}}$ [Ekström *et al.*, Phys. Rev. C **91**, 051301 (2015)] and the 1.8/2.0 (EM) [Hebel *et al.*, Phys. Rev. C **83**, 031301 (2011)]. We find that the effect of $3p$ - $3h$ excitations in the ground state is small for 1.8/2.0 (EM) but non-negligible for $\text{N}^2\text{LO}_{\text{sat}}$. The addition of these new correlations allows us to improve the precision of our ^{48}Ca calculations and reconcile the recently reported discrepancy between coupled-cluster results based on these interactions and the experimentally determined α_D from proton inelastic scattering in ^{48}Ca [Birkhan *et al.*, Phys. Rev. Lett. **118**, 252501 (2017)]. For the computation of electromagnetic and polarizability sum rules, the inclusion of leading-order $3p$ - $3h$ excitations in the ground state is important, while less so for the excited states and the similarity-transformed dipole operator.

PACS numbers: 21.60.De, 24.10.Cn, 24.30.Cz, 25.20.-x

I. INTRODUCTION

The electric dipole polarizability α_D has been measured in several nuclei [1–4], and is of key interest to theorists. On the one hand, mean-field calculations suggest that α_D is strongly correlated to the neutron skin, i.e. the difference between the root-mean-square (RMS) radii of the neutron and proton distributions [5–10], and thereby connects nuclei and neutron stars [11]. On the other hand, computations of ^{48}Ca by Hagen *et al.* [12] based on Hamiltonians from chiral effective field theory [13, 14] exhibit no correlations between the neutron skin and α_D , but do correlate the latter with both the RMS radius of the neutron distribution and the symmetry energy (and its slope) in nuclear matter, again providing a connection

between neutron-star physics and finite nuclei [15, 16]. The prediction [12] and measurement [4] of the dipole polarizability in ^{48}Ca agree within uncertainties, but theory somewhat overestimates the experimental data for some interactions. This motivates us to revisit this nucleus in this work, with an emphasis on computing α_D more precisely by going to the next level of approximation and include more many-body correlations.

We note that the study of the role of many-body correlations, while performed here with the coupled-cluster method [17–23], is relevant also for other methods such as self consistent Green's functions [24], in-medium similarity renormalization group [25, 26], and Gorkov-Green's function approaches [27]. All these methods seek economical ways to include the necessary particle-hole correlations required to achieve a precise calculation of energies and observables of ground- and excited states [28–30]. Thus, we expect that our results will also be useful for those applications.

In the last decade, major advancements have been made in first principles approaches to nuclear structure [23, 26, 31–35]. Realistic descriptions of nuclei as heavy as ^{78}Ni and ^{100}Sn have recently been achieved based on state-of-the-art nucleon-nucleon (NN) and three-nucleon forces (3NFs) from chiral effective field theory [36–38]. This advancement is based on the combination of first principles methods that scale polyno-

* This manuscript has been authored by UT-Battelle, LLC under Contract No. DE-AC05-00OR22725 with the U.S. Department of Energy. The United States Government retains and the publisher, by accepting the article for publication, acknowledges that the United States Government retains a non-exclusive, paid-up, irrevocable, world-wide license to publish or reproduce the published form of this manuscript, or allow others to do so, for United States Government purposes. The Department of Energy will provide public access to these results of federally sponsored research in accordance with the DOE Public Access Plan. (<http://energy.gov/downloads/doe-public-access-plan>).

mial with system size [19, 20, 24, 25, 39–45], an ever-increasing computational power following Moore’s law, insights from the renormalization group and effective field theory [46, 47], and progress with nuclear forces [48–51].

Electromagnetic reactions are a crucial tool to investigate nuclear dynamics [52–55], see Ref. [56] for a recent review. Due to the perturbative nature of the process, one can clearly separate the role of the known electromagnetic probe from the less well known nuclear dynamics. Through a comparison of experimental data with theory one is then able to assess the precision and accuracy of the employed nuclear interactions and associated current operators. Photo reactions on heavier nuclei can be computed by the combination of the Lorentz integral transform [57] and the coupled-cluster method [58–60], and by alternative means [30, 61–64].

A key ingredient to study electromagnetic reactions, such as photo-dissociation or electron scattering, is the nuclear response function, defined as

$$R(\omega, q) \equiv \sum_{\mu} \left| \langle \Psi_{\mu} | \hat{\Theta}(q) | \Psi_0 \rangle \right|^2 \delta(E_{\mu} - E_0 - \omega). \quad (1)$$

Here ω is the transferred energy, while $\hat{\Theta}(q)$ is the electromagnetic operator. It depends on the momentum-transfer q of the considered probe. The nuclear response function is a dynamical observable and requires knowledge of the ground state $|\Psi_0\rangle$ and all excited states $|\Psi_{\mu}\rangle$ with corresponding energies E_0 and E_{μ} , respectively. As most of the excited states are in the continuum, the sum in Eq. (1) really becomes an integral, and this makes the direct computation of the response function a formidable task.

Instead, it is often easier to compute sum rules of such response functions, i.e. moments of the response intended as a distribution function and defined as

$$m_n(q) \equiv \int_0^{\infty} d\omega \omega^n R(\omega, q). \quad (2)$$

Here, n is typically an integer. Employing the closure relation, we rewrite Eq. (2) as a ground-state expectation value

$$m_n = \langle \Psi_0 | \hat{\Theta}^{\dagger} (\hat{H} - E_0)^n \hat{\Theta} | \Psi_0 \rangle. \quad (3)$$

In practice, one often inserts completeness relations on the right of $\hat{\Theta}^{\dagger}$ and on the left of $\hat{\Theta}$, truncates the employed Hilbert spaces, and then increases the number of states until convergence is obtained.

While knowing the response function is equivalent to knowing all of its (existing) moments, already from a few moments one can gain useful insights into the dynamics of the nucleus. In this paper we will take this approach and focus on a few well known sum rules, namely the bremsstrahlung sum rule m_0 and the polarizability sum rule $\alpha_D \propto m_{-1}$ [see Eq. (6) below]. We calculate these observables within coupled-cluster theory using various

approximation levels, and infer information on the nuclear dynamics from a comparison to other available theoretical computations and/or experimental data.

In the long wave-length approximation, i.e., in the limit of $q \rightarrow 0$, the electric dipole operator reads

$$\hat{\Theta} = \sum_k^A (\mathbf{r}_k - \mathbf{R}_{\text{cm}}) \left(\frac{1 + \tau_k^3}{2} \right). \quad (4)$$

Here \mathbf{r}_k and \mathbf{R}_{cm} are the coordinates of the k -th nucleon and the center of mass of the nucleus, respectively, and τ_k^3 is the third component of the isospin operator. As an example, the photo-disintegration cross section of a nucleus below the pion production threshold becomes

$$\sigma_{\gamma}(\omega) = 4\pi^2 \alpha \omega R(\omega). \quad (5)$$

Here $R(\omega)$ is the response function (1) of the translationally invariant dipole operator (4) for $\omega = |\mathbf{q}|$. Employing an NN interaction from chiral effective field theory [65] this reaction cross section was calculated in Refs. [58, 59] using coupled-cluster theory with singles and doubles excitations (CCSD). While those calculations agreed with experimental data for ${}^4\text{He}$, ${}^{16-22}\text{O}$ and ${}^{40}\text{Ca}$, they lacked a better understanding of uncertainties related to the underlying Hamiltonian and the applied many-body approach.

The computation of a cross section or related sum rule exhibits various theoretical uncertainties. Often, the largest uncertainty results from truncations of the employed chiral effective field theory at some given order in the power counting, whereas statistical uncertainties due to the optimization of the interaction are significantly smaller [50, 66, 67]. While a robust quantification of systematic uncertainties related to the employed chiral interactions is still lacking, a rough estimate can be made by employing a large set of different chiral interactions [36, 48, 60, 68, 69]. Uncertainties from finite harmonic-oscillator basis can be estimated by varying the number of oscillator shells (N_{max}) and the oscillator frequency ($\hbar\Omega$). We found that this uncertainty is of the order of 1% for calculations in nuclei with mass number up to $A = 48$ [60]. Another source of uncertainty in the coupled-cluster method comes from truncating the cluster operator at some low-order particle-hole excitation rank. Previous works employed the CCSD approximation, and neglected higher order excitations, such as $3p$ - $3h$ excitations. It is the purpose of this paper to investigate the role of leading-order $3p$ - $3h$ excitations in the ground state, excited states, and the similarity transformed operator in the calculation of the bremsstrahlung sum rule m_0 [70–73] and on the electric dipole polarizability sum rule α_D [74].

The electric dipole polarizability is related to the inverse energy weighted sum rule m_{-1} as

$$\alpha_D = 2\alpha \int_{\omega_{\text{ex}}}^{\infty} d\omega \frac{R(\omega)}{\omega} = 2\alpha m_{-1}. \quad (6)$$

Due to the inverse energy weight, this sum rule is more sensitive to the low-energy part of the excitation spectrum.

This paper is organized as follows. In Section II we introduce the formalism used to calculate the response functions, and the sum rules m_0 and α_D . We also present the nomenclature used for the various approximation schemes that we implemented in this work. In Section III we present benchmarking results for m_0 and α_D in ${}^4\text{He}$ and ${}^{16}\text{O}$ to validate our approach. In Section IV, we revisit our ${}^{48}\text{Ca}$ calculations and compare them with the recent experimental data of Ref. [4]. Finally, we draw our conclusions in Section V.

II. THEORETICAL METHODS

Coupled-cluster theory [17, 19, 20, 22, 23, 40, 75–77] is based on the similarity transformed Hamiltonian,

$$\bar{H}_N = e^{-T} H_N e^T, \quad T = T_1 + T_2 + T_3 \dots \quad (7)$$

Here H_N is normal-ordered with respect to a single-reference state $|\Phi_0\rangle$ (usually the Hartree-Fock state), and T is an expansion in particle-hole excitations with respect to this reference. The similarity transformation decouples all particle-hole excitations from the ground state, and the reference state $|\Phi_0\rangle$ becomes the exact ground state of \bar{H}_N . In practice, the operator T is truncated at some low rank particle-hole excitation level. The similarity transformed Hamiltonian can be evaluated using the Baker-Campbell-Hausdorff expansion, and terminates exactly at quadruply nested commutators for a normal-ordered Hamiltonian containing at most up to two-body terms. The drawback from having an exactly terminating commutator expansion, is that the similarity transformed Hamiltonian is non-Hermitian and thus requires the computation of both the left and right eigenstates in order to evaluate expectation values and transitions. The left ground state is parameterized as

$$\langle \Psi_0 | = \langle \Phi_0 | (1 + \Lambda), \quad \Lambda = \Lambda_1 + \Lambda_2 + \Lambda_3 \dots, \quad (8)$$

where Λ is a sum of particle-hole de-excitation operators. The ground-state energy E_0 is given by the energy-functional

$$E_0 = E_{\text{HF}} + \langle \Phi_0 | (1 + \Lambda) \bar{H}_N | \Phi_0 \rangle. \quad (9)$$

Here E_{HF} is the Hartree-Fock reference energy. The left and right ground states are normalized according to $\langle \Phi_0 | (1 + \Lambda) | \Phi_0 \rangle = 1$.

For excited states we employ the equation-of-motion (EOM) coupled-cluster method [78] and calculate the right and left excited state of \bar{H}_N , i.e.,

$$\begin{aligned} \bar{H}_N R_\mu | \Phi_0 \rangle &= E_\mu R_\mu | \Phi_0 \rangle, \\ \langle \Phi_0 | L_\mu \bar{H}_N &= E_\mu \langle \Phi_0 | L_\mu. \end{aligned} \quad (10)$$

Here R_μ and L_μ are linear expansions in particle-hole excitations with

$$\begin{aligned} R_\mu &= r_0 + \sum_{i,a} r_i^a \hat{a}_a^\dagger \hat{a}_i + \frac{1}{(2!)^2} \sum_{i,j,a,b} r_{ij}^{ab} \hat{a}_a^\dagger \hat{a}_b^\dagger \hat{a}_j \hat{a}_i \\ &+ \frac{1}{(3!)^2} \sum_{i,j,k,a,b,c} r_{ijk}^{abc} \hat{a}_a^\dagger \hat{a}_b^\dagger \hat{a}_c^\dagger \hat{a}_k \hat{a}_j \hat{a}_i \\ &+ \frac{1}{(4!)^2} \sum_{i,j,k,l,a,b,c,d} r_{ijkl}^{abcd} \hat{a}_a^\dagger \hat{a}_b^\dagger \hat{a}_c^\dagger \hat{a}_d^\dagger \hat{a}_l \hat{a}_k \hat{a}_j \hat{a}_i \\ &+ \dots \end{aligned} \quad (11)$$

The expression for L_μ is equivalent. Here, \hat{a}^\dagger and \hat{a} are creation and annihilation operators, respectively. Indices a, b, c, d run over unoccupied orbitals, while i, j, k, l run over occupied orbitals. The left and right excited states are normalized according to

$$\langle \Phi_0 | L_\mu R_{\mu'} | \Phi_0 \rangle = \delta_{\mu, \mu'}. \quad (13)$$

The electromagnetic transition strength from the ground to an excited state is evaluated in coupled-cluster theory as

$$\begin{aligned} |\langle \Psi_\mu | \hat{\Theta} | \Psi_0 \rangle|^2 &= \langle \Psi_0 | \hat{\Theta}^\dagger | \Psi_\mu \rangle \langle \Psi_\mu | \hat{\Theta} | \Psi_0 \rangle = \\ &= \langle \Phi_0 | (1 + \Lambda) \bar{\Theta}_N^\dagger R_\mu | \Phi_0 \rangle \langle \Phi_0 | L_\mu \bar{\Theta}_N | \Phi_0 \rangle. \end{aligned} \quad (14)$$

Here $\bar{\Theta}_N \equiv e^{-T} \Theta_N e^T$ is the similarity transformed normal-ordered operator, which in this work is taken to be the electric dipole of Eq. (4). Because it is a one-body operator, the Baker-Campbell-Hausdorff expansion $\bar{\Theta}_N$ terminates at doubly nested commutators

$$\bar{\Theta}_N = \Theta_N + [\Theta_N, T] + \frac{1}{2} [[\Theta_N, T], T]. \quad (15)$$

Having defined the ground and excited states, we can rewrite the response function in the coupled-cluster formalism starting from Eq. (1) as

$$\begin{aligned} R(\omega) &= \sum_\mu \langle \Phi_0 | (1 + \Lambda) \bar{\Theta}_N^\dagger R_\mu | \Phi_0 \rangle \langle \Phi_0 | L_\mu \bar{\Theta}_N | \Phi_0 \rangle \\ &\times \delta(E_\mu - E_0 - \omega). \end{aligned} \quad (16)$$

By integrating over the energy ω we obtain the bremsstrahlung sum rule m_0

$$m_0 = \sum_\mu \langle \Phi_0 | (1 + \Lambda) \bar{\Theta}_N^\dagger R_\mu | \Phi_0 \rangle \langle \Phi_0 | L_\mu \bar{\Theta}_N | \Phi_0 \rangle. \quad (17)$$

Using the closure relation we obtain the equivalent expression

$$m_0 = \langle \Phi_0 | (1 + \Lambda) \bar{\Theta}_N^\dagger \cdot \bar{\Theta}_N | \Phi_0 \rangle. \quad (18)$$

In practice one solves for Eq. (18) by inserting a complete set on the Fock space defined by

$$1 = |\Phi_0\rangle \langle \Phi_0| + \sum_S |S\rangle \langle S| + \sum_D |D\rangle \langle D| + \sum_T |T\rangle \langle T| + \sum_Q |Q\rangle \langle Q| + \dots \quad (19)$$

Here S, D, T, Q label single, double, triple, and quadruple (and so on) excited reference states, corresponding to

$$\begin{aligned} \sum_S |S\rangle\langle S| &= \sum_{ia} |\Phi_i^a\rangle\langle\Phi_i^a|, \\ \sum_D |D\rangle\langle D| &= \sum_{ijab} |\Phi_{ij}^{ab}\rangle\langle\Phi_{ij}^{ab}|, \\ \sum_T |T\rangle\langle T| &= \sum_{ijkabc} |\Phi_{ijk}^{abc}\rangle\langle\Phi_{ijk}^{abc}|, \\ \sum_Q |Q\rangle\langle Q| &= \sum_{ijklabcd} |\Phi_{ijkl}^{abcd}\rangle\langle\Phi_{ijkl}^{abcd}|, \\ &\dots = \dots \end{aligned} \quad (20)$$

Here, $|\Phi_{i_1 \dots i_n}^{a_1 \dots a_n}\rangle = \hat{a}_{a_1}^\dagger \dots \hat{a}_{a_n}^\dagger \hat{a}_{i_n} \dots \hat{a}_{i_1} |\Phi_0\rangle$ is a np - nh state. Inserting the completeness (19) into Eq. (18) one obtains

$$\begin{aligned} m_0 &= \langle\Phi_0|(1+\Lambda)\bar{\Theta}_N^\dagger|\Phi_0\rangle\langle\Phi_0|\bar{\Theta}_N|\Phi_0\rangle \\ &= \sum_S \langle\Phi_0|(1+\Lambda)\bar{\Theta}_N^\dagger|S\rangle\langle S|\bar{\Theta}_N|\Phi_0\rangle \\ &+ \sum_D \langle\Phi_0|(1+\Lambda)\bar{\Theta}_N^\dagger|D\rangle\langle D|\bar{\Theta}_N|\Phi_0\rangle \\ &+ \sum_T \langle\Phi_0|(1+\Lambda)\bar{\Theta}_N^\dagger|T\rangle\langle T|\bar{\Theta}_N|\Phi_0\rangle \\ &+ \sum_Q \langle\Phi_0|(1+\Lambda)\bar{\Theta}_N^\dagger|Q\rangle\langle Q|\bar{\Theta}_N|\Phi_0\rangle + \dots \end{aligned} \quad (21)$$

Here the first term is identically zero for non-scalar operators $\hat{\Theta}$, such as the electric dipole operator considered in this work. Calculating m_0 from Eq. (21) is significantly simpler than starting from Eq. (17) since no knowledge of the excited states of \bar{H}_N is required. As a proof of principle we verified that solving Eq. (21) is equivalent to calculating the response function and integrating in ω using Eq. (17).

The inverse-energy-weighted-polarizability sum rule α_D of Eq. (6) can be calculated by utilizing the Lanczos continued fraction method [79] as

$$\begin{aligned} \alpha_D &= 2\alpha \langle\Phi_0|(1+\Lambda)\bar{\Theta}_N^\dagger \frac{1}{\bar{H}_N - E_0} \bar{\Theta}_N|\Phi_0\rangle \\ &= 2\alpha \mathcal{I}_L(\sigma=0, \Gamma=0) \\ &= m_0 x_{00}. \end{aligned} \quad (22)$$

Here $\mathcal{I}_L(\sigma, \Gamma)$ is the Lorentz integral transform, and x_{00} is a continued fraction of the Lanczos coefficients. To calculate the Lorentz integral transform [57, 58], one needs to solve an EOM with a source term and the non-symmetric Lanczos algorithm is implemented by constructing the right and left normalized pivots as (see Ref. [79] for details)

$$|P_r\rangle = \bar{\Theta}_N|\Phi_0\rangle, \quad (23)$$

$$\langle P_l| = m_0^{-1} \langle\Phi_0|(1+\Lambda)\bar{\Theta}_N^\dagger, \quad (24)$$

respectively.

So far we have not introduced any approximations in the coupled-cluster formulations for ground and excited states. The most commonly used approximation for the

ground state is CCSD (i.e. $T = T_1 + T_2$, and $\Lambda = \Lambda_1 + \Lambda_2$), which typically amounts for about 90% of the full correlation energy in systems with well defined single-reference character [21]. In the following we will denote the CCSD approximation in short with D. We will also go beyond the CCSD level by including leading-order $3p$ - $3h$ excitations using the CCSDT-1 approach [80]. CCSDT-1 is a good approximation to the full CCSDT approach and accounts for about 99% of the correlation energy. In brief, CCSDT-1 is an iterative approach that includes the leading-order contribution $(H_N T_2)_C$ (here the index C denotes that only connected terms contribute [81]) to the T_3 amplitudes with an energy denominator given by the Hartree-Fock single-particle energies, while all T_3 contributions to the T_1 and T_2 amplitudes are fully included. We will also solve for the corresponding left ground state in the CCSDT-1 following Ref. [82]. To simplify the notation, in the following we will label the CCSDT-1 approximation with T-1. The corresponding approximations we will employ for excited states given in Eq. (10) includes up to $2p$ - $2h$ in the EOM-CCSD approach, and leading-order $3p$ - $3h$ excitations in the EOM-CCSDT-1 approach [82, 83]. Because the calculation of the ground state α_D requires a particle-hole expansion of the ground state (T and Λ) and one for excited states $[R_\mu$ and L_μ for α_D or Eq. (21) for $m_0]$, we need to label both of them appropriately. In this work we will investigate different approximation levels in both the ground and excited states. In order to keep the notation concise we therefore denote each scheme with a pair of labels (separated by a '/' symbol), with the largest order of correlation included in the ground state on the left, and the largest order of correlation included in the excited states on the right as shown in Table I. In the previous work on dipole strengths and polarizabilities [4, 58–60, 79] both ground and excited states were approximated at the CCSD level, an approximation we label by D/D in this work.

TABLE I. List of labels to denote the various coupled-cluster expansions used for the ground state (left of '/') and for the excited states (right of '/'). The symbol (S for singles, D for doubles, T for triples and T-1 for linearized triples) represents the highest order of correlation considered (with all lower orders always fully included).

ground state	EOM	label
D	S	D/S
D	D	D/D
T-1	S	T-1/S
T-1	D	T-1/D
T-1	T-1	T-1/T-1

Examining the similarity transformed one-body operator $\bar{\Theta}_N$ of Eq. (15) reveals that for $T = T_1 + T_2$, the expansions of Eqs. (21) and (22) terminate at triply excited determinants ($|T\rangle$). If one includes $T = T_1 + T_2 + T_3$

the expansions terminate at quadruply excited determinants. Thus, the inclusion of $3p$ - $3h$ excitations in the ground and excited states requires the implementation of a number of new coupled-cluster diagrams. As usual, we checked such diagrams by comparing the j -coupling and m -coupling schemes (see, e.g., Ref. [84]).

III. VALIDATION AND BENCHMARKING

For a validation of our approach, we benchmark our results on ${}^4\text{He}$ and ${}^{16}\text{O}$. In all the results presented in this Section, ${}^4\text{He}$ is calculated with the the chiral NN interaction at next-to-next-to-next-to-leading order ($N^3\text{LO}$) from Ref. [65], and ${}^{16}\text{O}$ is calculated using the $N^2\text{LO}_{\text{sat}}$ interaction [48], respectively. The choice of interaction for ${}^4\text{He}$ is motivated by the fact that we want to benchmark the various approximation schemes against virtually exact results from the effective hyperspherical harmonics approach [85], which cannot easily employ the $N^2\text{LO}_{\text{sat}}$ due to the non-locality of the 3NF. For ${}^{16}\text{O}$, the inclusion of 3NFs is necessary for a realistic description of the charge radius and observables correlated with it, such as m_0 and α_D [4, 60, 79]. This makes the interaction $N^2\text{LO}_{\text{sat}}$ a good choice. Using this interaction also allows us to benchmark with self consistent Green's function results [30].

We first explore how the similarity-transformed transition operator depends on the truncation level of included triples excitations. Then we compute the m_0 sum rule and the dipole polarizability for ${}^4\text{He}$ and ${}^{16}\text{O}$. For ${}^{16}\text{O}$ we also show a comparison of running sum rules and discretized responses, which allow us to monitor how excited states move as a function of energy for the various approximation schemes.

A. The similarity transformed transition operator

In the T-1/S, T-1/D, and T-1/T-1 approaches, T_3 contributions are included in the one- and two-body parts of the similarity transformed Hamiltonian, while three-body parts from T_3 are only included via $(F_N T_3)_C$ (here F_N is the normal ordered one-body Fock matrix). By treating the similarity transformation of a normal-ordered one-body operator $\hat{\Theta}_N$ consistently with the similarity-transformed Hamiltonian, one has

$$\begin{aligned} \bar{\Theta}_N &= [\Theta_N e^{T_1+T_2+T_3}]_C = \\ &= \bar{\Theta}_N^D + \left[\Theta_N \left(\frac{T_2^2}{2} + T_3 + T_1 T_3 \right) \right]_C \end{aligned} \quad (25)$$

$$\simeq \bar{\Theta}_N^D + \left[\Theta_N \left(\frac{T_2^2}{2} \right) \right]_C \quad (26)$$

$$\simeq \bar{\Theta}_N^D, \quad (27)$$

where the C index again denotes connected diagrams [81] and $\bar{\Theta}_N^D$ is the similarity-transformed operator in the D

approximation. Due to the hierarchy among correlations, one can expect that the terms in Eq. (25) that contain T_3 are sub-leading with respect to the T_2^2 term. These terms are also computationally much more demanding since they involve calculating and storing T_3 configurations (see Ref. [84] for full expressions). Thus, it is convenient to explore their relevance with respect to using Eq. (26), or even just using Eq. (27), where the operator is similarity transformed as in the D approximation.

In this paper we compute observables by including $3p$ - $3h$ excitations in the ground and excited states as well as in the similarity transformed operator, and benchmark the various approximations for $\bar{\Theta}_N$ in ${}^4\text{He}$ and ${}^{16}\text{O}$, as shown in Table II. We see that for both m_0 and α_D , the additional terms in Eqs. (25) and (26) have a negligible contribution with respect to Eq. (27), amounting to a sub-percent effect of about 0.2 and 0.7%, respectively. This finding is important in the light of performing computations of heavy nuclei, where calculations with Eq. (27) are more tractable, while using Eq. (25) would be substantially more computationally demanding. Consequently, when calculating ${}^{48}\text{Ca}$ in Section IV, we will use Eq. (27).

TABLE II. Effect of contributions of $3p$ - $3h$ correlations in a T-1/T-1 computation, when $\bar{\Theta}_N$ is truncated as in Eqs. (25) or (26), with respect to the full expression of Eq. (27). Both m_0 and α_D are computed with (a) $\hbar\Omega = 26$ MeV and $N_{\text{max}} = 14$ and (b) $\hbar\Omega = 22$ MeV, $N_{\text{max}} = 12$ and $E_{3\text{max}}^F = 14$.

	${}^4\text{He}^{(a)}$	${}^{16}\text{O}^{(b)}$	scheme
$m_0[\text{fm}^2]$	0.951	4.87	Eq. (25)
	0.950	4.92	Eq. (26)
	0.949	4.90	Eq. (27)
$\alpha_D[\text{fm}^3]$	0.0816	0.523	Eq. (25)
	0.0808	0.528	Eq. (26)
	0.0811	0.527	Eq. (27)

Note that when using Eq. (27) in the calculation of m_0 in the T-1/T-1 approximation, $3p$ - $3h$ excitations enter only in the ground state [see Eq. (18)], and therefore this corresponds to the T-1/D approximation. On the contrary, triples would enter both in the ground and excited states in a calculation of α_D , for which T-1/T-1 and T-1/D are different.

B. ${}^4\text{He}$

We now focus on ${}^4\text{He}$ and explore the convergence in terms of the model space size N_{max} for two approximation schemes that includes $3p$ - $3h$ excitations, namely T-1/T-1 and T-1/D, and compare it to the D/D approximation.

Fig. 1 shows the convergence of m_0 and α_D in ${}^4\text{He}$ with respect to N_{max} for $\hbar\Omega = 26$ MeV. Calculations in the T-

1/T-1 and T-1/D scheme were performed with Eq. (26) and Eq. (27), respectively. The convergence with respect to N_{\max} is of similar quality both for m_0 (a) and α_D (b).

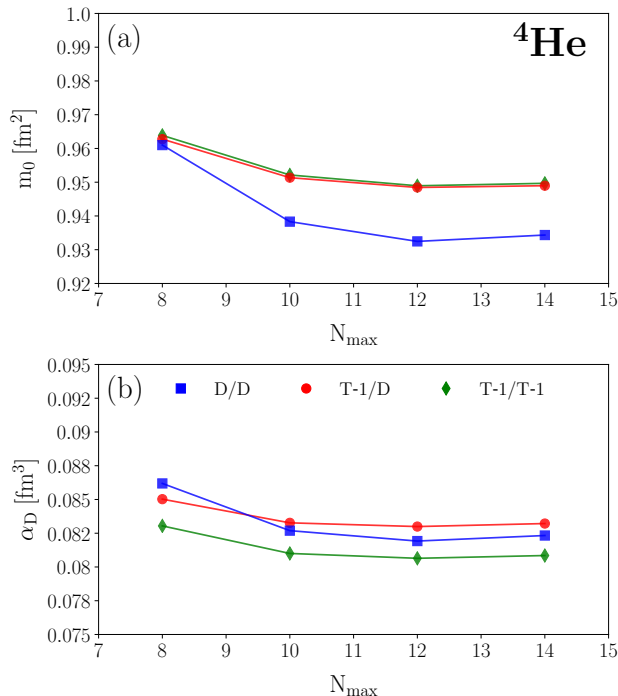


FIG. 1. (Color online) Convergence of m_0 (a) and α_D (b) for ^4He with respect to the model-space size N_{\max} for $\hbar\Omega = 26$ MeV. Two triples approximations schemes T-1/T-1 (green diamonds) and T-1/D (red circles) are compared to the D/D case (blue squares). The similarity transformed operator is implemented with Eq. (26) and (27), in T-1/T-1 and T-1/D, respectively.

We see that for m_0 , the results obtained within the T-1/D approximation are close to those obtained in T-1/T-1 approximation. The slight difference stems from the fact that the T-1/T-1 calculations are performed with the similarity transformed operator given in Eq. (26), while T-1/D results are obtained with Eq. (27). We implement these two different equations to graphically show that our findings presented in Table II are consistent in various model spaces and approximations. For α_D we observe a slightly larger difference between the T-1/T-1 and T-1/D approximations, due to the fact that $3p-3h$ excitations enter in the calculations of excited states as well. Overall, the effects of $3p-3h$ excitations in ^4He are small, amounting to about 1.5%.

It is now interesting to compare the various coupled-cluster results with respect to the hyperspherical harmonics benchmark values [58, 85] for ^4He . Figure 2 shows m_0 (a) and α_D (b) obtained for various approximations in coupled-cluster theory: D/D (blue/left), the T-1/D (red/central) and the T-1/T-1 (green/right). The widths of the bands reflect the residual $\hbar\Omega$ dependence for the largest model space $N_{\max} = 14$. The black line is the vir-

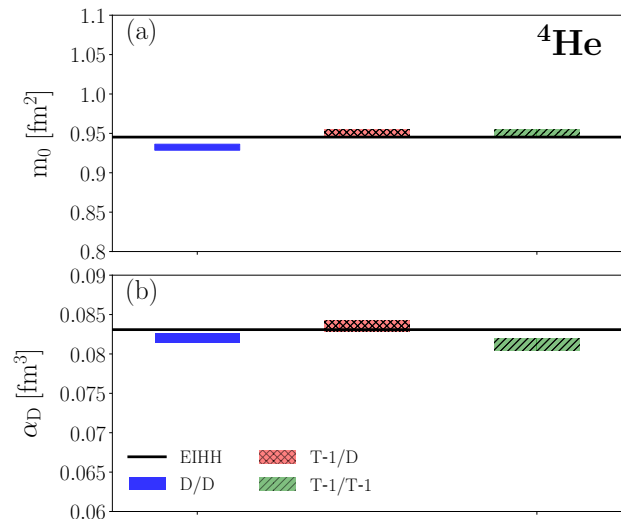


FIG. 2. (Color online) Comparison of m_0 (a) and α_D (b) in the D/D (blue/left), the T-1/D (red/central) and the T-1/T-1 (green/right) approximations against hyperspherical harmonics results (black line) in ^4He .

tually exact calculation from hyperspherical harmonics expansions using the same interaction. The D/D calculations already get close to the hyperspherical harmonics result, and the addition of $3p-3h$ correlations in both the T-1/D and T-1/T-1 approaches further improves the agreement for m_0 . For α_D the T-1/D calculation agrees better with the hyperspherical harmonics result than the T-1/T-1 approach. The overall effect of $3p-3h$ excitations is small. This benchmark with hyperspherical harmonics suggests that the T-1/D scheme is to be preferred for electromagnetic and polarizability sum rules, and that the inclusion of $3p-3h$ correlations in the ground state plays a more significant role than the corresponding one in the excited states.

C. ^{16}O

Let us turn to ^{16}O . First, we check the convergence of the m_0 sum rule with respect to the number of $3p-3h$ configurations included in our calculations. Going beyond the D/D approximation and including $3p-3h$ excitations in the T-1/S, T-1/D, and T-1/T-1 approaches, the computational cost grows significantly both in terms of number of computational cycles and memory associated with storage of the amplitudes. The computational cost associated with the most expensive term in the D/D approximation is given by $n_o^2 n_u^4$, while in the T-1/S, T-1/D, and T-1/T-1 approaches it is $n_o^3 n_u^4$. Here n_o is the number of occupied orbitals in the reference state $|\Phi_0\rangle$ and n_u is the number of unoccupied orbitals. Clearly, the computational load grows rapidly with the mass of the nucleus ($n_o = A$) and the model-space size ($n_u \propto N_{\max}^3$). In or-

der to overcome this computational hurdle in the T-1/S, T-1/D, and T-1/T-1 approaches, we introduce an energy cut $E_{3\max}^F$ on the allowed $3p$ - $3h$ excitations. The truncated space that we employ for the $3p$ - $3h$ excitations are thus given by $|N_a - N_F| + |N_b - N_F| + |N_c - N_F| \leq E_{3\max}^F$ and $|N_i - N_F| + |N_j - N_F| + |N_k - N_F| \leq E_{3\max}^F$ with $N_p = 2n_p + l_p$ being the harmonic-oscillator shell and N_F the harmonic-oscillator shell at the Fermi surface. The top of Fig. 3 shows the convergence with respect to $E_{3\max}^F$ for m_0 in ^{16}O . We observe that truncating $E_{3\max}^F$ to 14 yield results for ^{16}O that are converged at the 1%-level. Unless stated otherwise, in the remainder of this work we will use $E_{3\max}^F = 14$. Note that this truncation also works well for ^{48}Ca , as shown in the bottom part of Fig. 3.

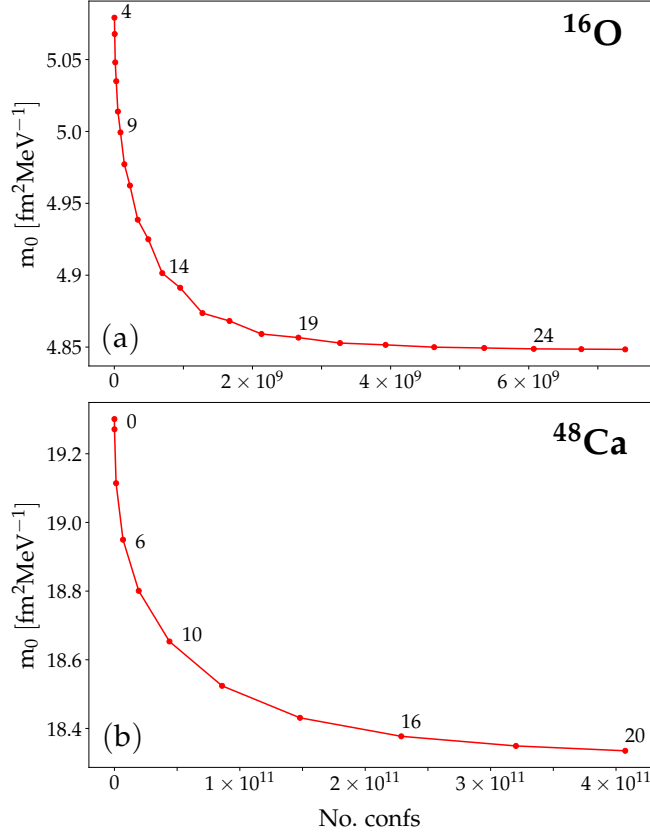


FIG. 3. (Color online) Convergence of m_0 for ^{16}O (a) and ^{48}Ca (b) calculated in the T-1/D scheme as a function of the number of configurations for the $E_{3\max}^F$. The adopted model space is $N_{\max} = 12$. Each point corresponds to a jump of one unit (two units) in $E_{3\max}^F$ for ^{16}O (^{48}Ca) and selected values of $E_{3\max}^F$ are highlighted along the curves.

In Fig. 4 we show results for the m_0 sum rule (top) and the dipole polarizability (bottom) of ^{16}O at $\hbar\Omega = 22$ MeV and $E_{3\max}^F = 14$ as a function of N_{\max} . For m_0 , the T-1/T-1 and T-1/D calculations almost coincide, while some difference is observed in α_D . The residual $\hbar\Omega$ dependence amounts to about 1.5% in the largest model space. While in ^{16}O the effect of triples is slightly

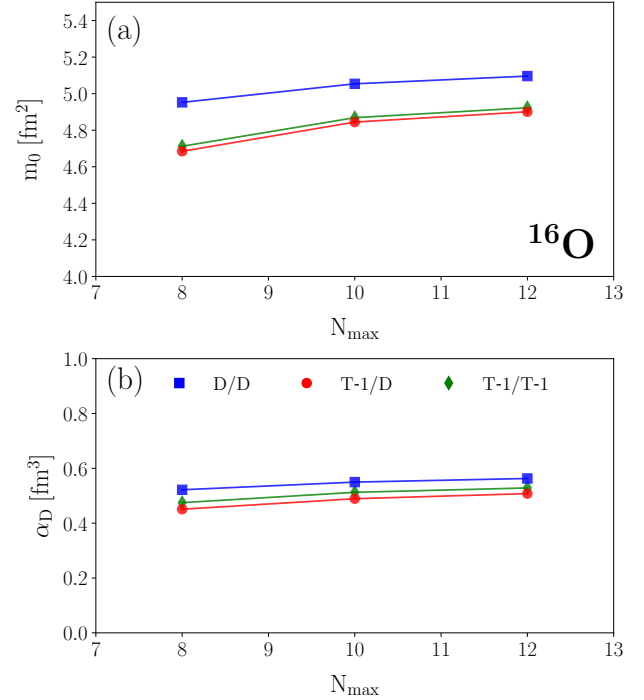


FIG. 4. (Color online) Convergence of m_0 (a) and α_D (b) for ^{16}O with respect to the model-space size N_{\max} for $\hbar\Omega = 22$ MeV and $E_{3\max}^F = 14$. Two triples approximations schemes T-1/T-1 (green diamonds) and T-1/D (red circles) are compared to the D/D case (blue squares). The similarity transformed operator is implemented with Eq. (26) and (27), in T-1/T-1 and T-1/D, respectively.

larger than in ^4He , the overall effect of $3p$ - $3h$ excitations is small and amounts to 4% and 6% for m_0 and α_D , respectively. Both for m_0 and α_D the inclusion of $3p$ - $3h$ excitations in the T-1/T-1 and T-1/D approaches reduce their magnitude as compared to the results obtained in the D/D approach.

In Fig. 5 we compare m_0 (a) and α_D (b) for ^{16}O obtained in the D/D (blue/right) scheme with the T-1/D (red/central) and the T-1/T-1 (green/right) approximations. The D/D value is obtained at $N_{\max} = 14$ and $\hbar\Omega = 22$ MeV. Due to the large number of $3p$ - $3h$ configurations, for ^{16}O we are able to calculate only up to a maximum model space of $N_{\max} = 12$ and $E_{3\max}^F = 14$ for T-1/T-1. For consistent results we adopt the same truncation for $E_{3\max}^F$ in T-1/D. The bands in Fig. 5 are obtained by assigning a 2% uncertainty, accounting for the combined uncertainty from the $E_{3\max}^F$ cut and the residual $\hbar\Omega$ -dependence.

Correlations arising from $3p$ - $3h$ excitations reduce the size of these observables by a few percent, with effects being slightly larger on α_D than for m_0 . Similar to the ^4He case, we find that results for m_0 obtained in the T-1/D and T-1/T-1 approaches almost coincide, while for α_D they slightly differ. This is expected, because m_0

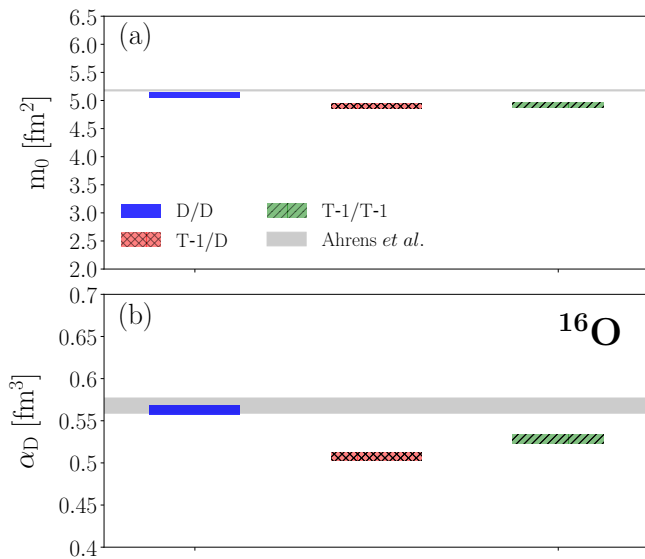


FIG. 5. (Color online) Comparison of m_0 (a) and α_D (b) in the D/D (blue/left), the T-1/D (red/central) and the T-1/T-1 (green/right) approximations against the integrated experimental data by Ahrens *et al.* [86] in ^{16}O .

is calculated as a ground-state expectation value, while α_D also requires the solution of the excited states from Eq. (10). We use the difference between the T-1/D and T-1/T-1 results as an estimate of neglected higher order correlations. This amounts to a 4% effect for α_D and an even smaller effect of 0.4% for m_0 .

We now confront our results with data. Figure 5 compares the theoretical results with the experimental value obtained by integrating the data from Ahrens *et al.* [86] (grey bands). We see that the addition of triples leads to a deviation of m_0 and α_D with respect to the experimental data, which agreed better in the D/D approximation using the $\text{N}^2\text{LO}_{\text{sat}}$ interaction. We note that $\text{N}^2\text{LO}_{\text{sat}}$ was constrained to reproduce the charge radius of ^{16}O using coupled-cluster theory in the D approximation. As shown in Refs. [12, 79], the charge radius is correlated with α_D , and it would therefore be interesting to quantify the effect of $3p$ - $3h$ excitations in the T-1 approach on charge radii as well. We also note that the extraction of these sum rules from photo-absorption data may be prone to larger systematic uncertainties than those quoted because it is not possible to estimate the role of multipoles beyond the dipole.

As the experimental determination of the dipole polarizability results from an integration of the dipole strength, it is interesting to study the running of the α_D sum rules as a function of the maximum integration limit. If one solves for the excited states in Eq. (10) using the Lanczos technique, it is possible to define the sum rule from the integral of the dipole response function $R(\omega)$ as

$$m_n(\varepsilon) = \int_0^\varepsilon d\omega \omega^n R(\omega), \quad (28)$$

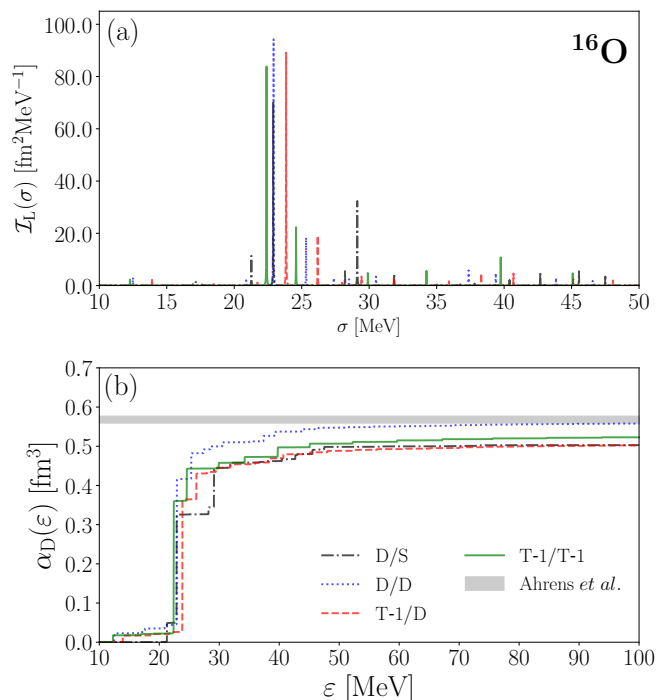


FIG. 6. (Color online) Discretized response with $\Gamma = 0.01$ MeV (a) and running sum of $\alpha_D(\varepsilon)$ (b) for ^{16}O with various coupled-cluster approximations compared with experimental results from Ahrens *et al.* [86].

and study its running as a function of ε . A discretized response function can also be obtained by a calculation of the Lorentz integral transform $\mathcal{I}_L(\sigma, \Gamma)$ [57, 58] for a very small width parameter Γ as (see Ref. [79] for details)

$$m_n(\varepsilon) = \lim_{\Gamma \rightarrow 0} \int_0^\varepsilon d\sigma \sigma^n \mathcal{I}_L(\sigma, \Gamma). \quad (29)$$

The discretized response consists of smeared δ peaks and does not properly take the continuum into account. However, it will allow us to see how excited states and their corresponding strengths change within various approximation schemes, thus affecting the running sums.

The top of Fig. 6 shows the Lorentz integral transform calculated for $\Gamma = 0.01$ MeV using various coupled-cluster approximations for ^{16}O . The bottom plot shows the running of the polarizability sum rule as a function of ε . The various approximation schemes are shown in comparison with experimental data (gray bands). Besides the D/D calculation, we present three different schemes with increasing correlation order, namely D/S, T-1/D and T-1/T-1. We note that the D/S scheme coincides with the T-1/D calculation, and is also very close to the most expensive T-1/T-1 calculation, deviating from the D/D approximation by a few percent.

In Table III we compare our results for α_D with those of Barbieri *et al.* [30]. We see that the results obtained with the D/S approach agree with calculations from the self consistent Green's functions method that used a

TABLE III. Comparison of coupled-cluster results with self consistent Green’s function data from Ref. [30] in ^{16}O using the $\text{N}^2\text{LO}_{\text{sat}}$ interaction.

Method	α_D [fm^3]
Ref. [30]	0.50
D/S	0.503
T-1/D	0.508
T-1/T-1	0.528

random phase approximation approach for the excited states. We find that the inclusion of $3p$ - $3h$ correlations in the ground state and in the excited states decreases the polarizability with respect to a D/D calculation, making this more sophisticated calculation to coincidentally agree with simpler schemes, such as the D/S approximation.

IV. ELECTRIC DIPOLE POLARIZABILITY OF ^{48}Ca

We now turn to our main goal and compute the dipole polarizability of ^{48}Ca . In the recent experiment using proton inelastic scattering off a ^{48}Ca target, the electric dipole strength was disentangled from other multipole contributions resulting in $\alpha_D = 2.07(22) \text{ fm}^3$ [4]. Overall, theory agreed with experiment, given the (still significant) systematic theoretical uncertainties as one varies the employed interaction. However, calculations based on interactions that reproduced the charge radius of ^{48}Ca yielded results for α_D in the D/D approximation that were somewhat larger than the measured value. Those calculations were performed in the D/D approximation, and this makes it interesting to compute α_D with an increased precision by including leading-order $3p$ - $3h$ correlations in the T-1 approximation.

Taking advantage of the results and benchmarks from Section III, we revisit these calculations by using two established interactions, namely $\text{N}^2\text{LO}_{\text{sat}}$ and 1.8/2.0 (EM). These two interactions were also used in Refs. [4, 12]. The 1.8/2.0 (EM) potential is constructed following Ref. [87]. It starts from the chiral NN interaction at N^3LO [65] and “softens” it with the similarity renormalization group [47] at a cutoff/resolution scale $\lambda_{\text{SRG}} = 1.8 \text{ fm}^{-1}$. The 3NF is taken as the leading chiral 3NF using a non-local regulator and cutoff $\lambda_{3\text{NF}} = 2.0 \text{ fm}^{-1}$, with short-ranged coefficients c_D and c_E adjusted to $A \leq 4$ nuclei. The “1.8/2.0 (EM)” interaction reproduces binding energies and spectra in medium-mass and heavy nuclei [36–38], but yields too small charge radii. The $\text{N}^2\text{LO}_{\text{sat}}$ interaction yields radii in better agreement with data.

Figure 7 shows the m_0 sum rule (top) and the dipole polarizability α_D (bottom) obtained in the D/D and

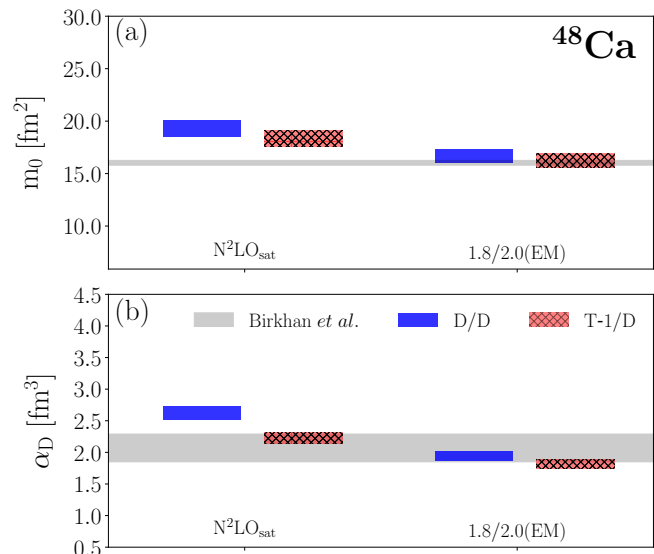


FIG. 7. (Color online) Comparison of m_0 (a) and α_D (b) in the D/D (blue/left) and the T-1/D (red/right) approximations in ^{48}Ca . Results for the $\text{N}^2\text{LO}_{\text{sat}}$ (leftmost bands) and 1.8/2.0 (EM) (rightmost bands) interactions are shown. For the polarizability the results are compared against experimental data by Birkhan *et al.* [4].

T-1/D approaches using the $\text{N}^2\text{LO}_{\text{sat}}$ (leftmost bands) and 1.8/2.0 (EM) (rightmost bands) interactions, respectively. The grey horizontal bands are data. For $\text{N}^2\text{LO}_{\text{sat}}$ we find that the addition of $3p$ - $3h$ excitations in the ground state using the T-1 approach improves the agreement with the data. As calculations of excited states in the T-1 approach are computationally demanding and currently not feasible at sufficiently large $E_{3\text{max}}^F$ cut, we did not employ the T-1/T-1 approach for ^{48}Ca . However, based on our studies for ^4He and ^{16}O one may expect that the T-1/D and T-1/T-1 approaches would yield similar results.

We observe that both for m_0 and α_D the T-1 approximation for the ground state leads to a reduction of the strength, bringing theory in agreement with the recent data from Birkhan *et al.* [4]. Remarkably, the inclusion of leading triples corrections also reduces the Hamiltonian model dependence, leading to a more precise calculation of m_0 and α_D . The effect of the triples on α_D amounts to 15% for the $\text{N}^2\text{LO}_{\text{sat}}$ and 6% for the 1.8/2.0 (EM) interaction, which is consistent with the latter being a much “softer” interaction. The triples effect on m_0 is smaller, amounting to about 5% for $\text{N}^2\text{LO}_{\text{sat}}$ and 2% for the 1.8/2.0 (EM) interaction. We also performed T-1 calculations for the charge radius of ^{48}Ca , and found that inclusion of triples excitations increases the radius by about 1% for both the 1.8/2.0 (EM) and $\text{N}^2\text{LO}_{\text{sat}}$ interactions as compared to the D approximation. Thus, the effect of triples excitations on the charge radius of ^{48}Ca is negligible, and the results and conclusions of Ref. [48] are accurate.

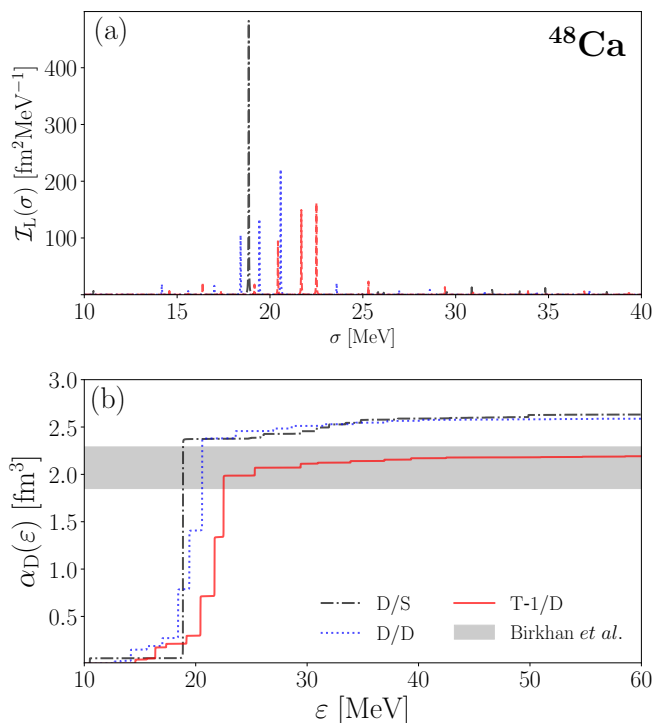


FIG. 8. (Color online) Discretized response with $\Gamma = 0.01$ MeV (a) and running sum of $\alpha_D(\varepsilon)$ (b) for ^{48}Ca with various coupled-cluster approximations compared with experimental results from Birkhan *et al.* [4]

Figure 8 shows the Lorentz integral transform (top) calculated for $\Gamma = 0.01$ MeV using various coupled-cluster approximations, and the running of the polarizability sum rule as a function of ε (bottom). The various approximation schemes are shown in comparison with experimental data (gray bands). Besides the D/D calculation, we present three different schemes with increasing correlation order, namely D/S, T-1/D and T-1/T-1.

Interestingly, for ^{48}Ca we see that for the D/S approximation the strength is dominated by a single state at around 19 MeV of excitation energy, while higher-order correlations included in D/D and T-1/D shift and fragment the strength significantly. The inclusion of $3p$ - $3h$ excitations via the T-1 approach in the ground state, makes the strength more fragmented and also increases some of the strength at higher energy. Such fragmentation combined with the inverse energy weight in the polarizability sum rule is the mechanisms that leads to a reduction of α_D . Opposite to what was found in ^{16}O , for ^{48}Ca the computationally least expensive D/S approximation coincidentally agrees with D/D and not with the computationally most expensive approximation (T-1/D in this case).

V. CONCLUSIONS

We computed the electric dipole polarizability α_D of ^{48}Ca with an increased precision by including leading $3p$ - $3h$ correlations. Leading order $3p$ - $3h$ excitations were implemented in the CCSDT-1 approximation for the ground state, excited states, and the similarity transformed dipole operator. The effect of $3p$ - $3h$ excitations on the latter was found to be negligible. The inclusion of $3p$ - $3h$ excitations in the ground state via CCSDT-1 is sufficient to obtain an agreement with the hyperspherical harmonics approach for ^4He to better than 1%. While the effect of triples is quite small in ^4He , it becomes larger in ^{16}O and ^{48}Ca . In ^{16}O triples excitations reduce the size of m_0 sum rule and α_D by about 4-6%. In ^{48}Ca they reduce α_D by about a 15% reduction for the $\text{N}^2\text{LO}_{\text{sat}}$ interaction and by about 6% for the 1.8/2.0 (EM) interaction. This brings our coupled-cluster calculations in agreement with the recent experimental result obtained from inelastic proton scattering [4]. The effect of triples excitations is smaller for the m_0 sum rule in ^{48}Ca , and reduces it by about 5% and 2% for the two interactions considered, respectively. Finally we found that the effect of triples excitations on the charge radius of ^{48}Ca is negligible, and increases it by about 1% for both interactions considered in this work.

We note that some simpler approximations may occasionally coincide with more sophisticated computations using the CCSDT-1 method both for the ground and excited states. We conclude that the effect of $3p$ - $3h$ excitations in the ground state is more important than their effect in excited states for the electromagnetic sum rules studied in this work. The inclusion of triples excitations in the excited states, while possible for light nuclei such as ^4He and ^{16}O , will require further developments in order to overcome the hurdles associated with the increase in computational cost for heavier nuclei. We expect our results also to be relevant for other many-body approaches, such as the self consistent Green's function and the in medium similarity renormalization group methods.

ACKNOWLEDGMENTS

This work was supported in parts by the Natural Sciences and Engineering Research Council (NSERC), the National Research Council of Canada, by the Deutsche Forschungsgemeinschaft DFG through the Collaborative Research Center [The Low-Energy Frontier of the Standard Model (SFB 1044)], and through the Cluster of Excellence [Precision Physics, Fundamental Interactions and Structure of Matter (PRISMA)], by the Office of Nuclear Physics, U.S. Department of Energy under Grants Nos. DE-FG02-96ER40963 (University of Tennessee) de-sc0008499 (SciDAC-3 NUCLEI), de-sc0018223 (SciDAC-4 NUCLEI), and the Field Work Proposals ERKBP57 and ERKBP72 at Oak Ridge National Laboratory. Computer time was provided by the Innovative and Novel

Computational Impact on Theory and Experiment (IN-CITE) program. This research used resources of the Oak Ridge Leadership Computing Facility located in the Oak Ridge National Laboratory, supported by the Office of Science of the U.S. Department of Energy under Contract

No. DE-AC05-00OR22725, and computational resources of the National Center for Computational Sciences, the National Institute for Computational Sciences, and TRIUMF.

-
- [1] A. Tamii, I. Poltoratska, P. von Neumann-Cosel, Y. Fujita, T. Adachi, C. A. Bertulani, J. Carter, M. Dozono, H. Fujita, K. Fujita, K. Hatanaka, D. Ishikawa, M. Itoh, T. Kawabata, Y. Kalmykov, A. M. Krumbholz, E. Litvinova, H. Matsubara, K. Nakanishi, R. Neveling, H. Okamura, H. J. Ong, B. Özel-Tashenov, V. Yu. Ponomarev, A. Richter, B. Rubio, H. Sakaguchi, Y. Sakemi, Y. Sasamoto, Y. Shimbara, Y. Shimizu, F. D. Smit, T. Suzuki, Y. Tameshige, J. Wambach, R. Yamada, M. Yosoi, and J. Zenihiro, “Complete electric dipole response and the neutron skin in ^{208}Pb ,” *Phys. Rev. Lett.* **107**, 062502 (2011).
- [2] D. M. Rossi, P. Adrich, F. Aksouh, H. Alvarez-Pol, T. Aumann, J. Benlliure, M. Böhmer, K. Boretzky, E. Casarejos, M. Chartier, A. Chatillon, D. Cortina-Gil, U. Datta Pramanik, H. Emling, O. Ershova, B. Fernandez-Dominguez, H. Geissel, M. Gorska, M. Heil, H. T. Johansson, A. Junghans, A. Kelic-Heil, O. Kiselev, A. Klimkiewicz, J. V. Kratz, R. Krücken, N. Kurz, M. Labiche, T. Le Bleis, R. Lemmon, Yu. A. Litvinov, K. Mahata, P. Maierbeck, A. Movsesyan, T. Nilsson, C. Nociforo, R. Palit, S. Paschalis, R. Plag, R. Reifarth, D. Savran, H. Scheit, H. Simon, K. Sümmerer, A. Wagner, W. Waluś, H. Weick, and M. Winkler, “Measurement of the dipole polarizability of the unstable neutron-rich nucleus ^{68}Ni ,” *Phys. Rev. Lett.* **111**, 242503 (2013).
- [3] T. Hashimoto, A. M. Krumbholz, P.-G. Reinhard, A. Tamii, P. von Neumann-Cosel, T. Adachi, N. Aoi, C. A. Bertulani, H. Fujita, Y. Fujita, E. Ganioglu, K. Hatanaka, E. Ideguchi, C. Iwamoto, T. Kawabata, N. T. Khai, A. Krugmann, D. Martin, H. Matsubara, K. Miki, R. Neveling, H. Okamura, H. J. Ong, I. Poltoratska, V. Yu. Ponomarev, A. Richter, H. Sakaguchi, Y. Shimbara, Y. Shimizu, J. Simonis, F. D. Smit, G. Süsoy, T. Suzuki, J. H. Thies, M. Yosoi, and J. Zenihiro, “Dipole polarizability of ^{120}Sn and nuclear energy density functionals,” *Phys. Rev. C* **92**, 031305 (2015).
- [4] J. Birkhan, M. Miorelli, S. Bacca, S. Bassauer, C. A. Bertulani, G. Hagen, H. Matsubara, P. von Neumann-Cosel, T. Papenbrock, N. Pietralla, V. Yu. Ponomarev, A. Richter, A. Schwenk, and A. Tamii, “Electric dipole polarizability of ^{48}Ca and implications for the neutron skin,” *Phys. Rev. Lett.* **118**, 252501 (2017).
- [5] R. J. Furnstahl, “Neutron radii in mean-field models,” *Nuclear Physics A* **706**, 85 – 110 (2002).
- [6] P.-G. Reinhard and W. Nazarewicz, “Information content of a new observable: The case of the nuclear neutron skin,” *Phys. Rev. C* **81**, 051303 (2010).
- [7] X. Roca-Maza, M. Centelles, X. Viñas, and M. Warda, “Neutron skin of ^{208}Pb , nuclear symmetry energy, and the parity radius experiment,” *Phys. Rev. Lett.* **106**, 252501 (2011).
- [8] J. Piekarewicz, B. K. Agrawal, G. Colò, W. Nazarewicz, N. Paar, P.-G. Reinhard, X. Roca-Maza, and D. Vretenar, “Electric dipole polarizability and neutron skin,” *Phys. Rev. C* **85**, 041302 (2012).
- [9] X. Roca-Maza, M. Brenna, G. Colò, M. Centelles, X. Viñas, B. K. Agrawal, N. Paar, D. Vretenar, and J. Piekarewicz, “Electric dipole polarizability in ^{208}Pb : Insights from the droplet model,” *Phys. Rev. C* **88**, 024316 (2013).
- [10] P.-G. Reinhard, J. Piekarewicz, W. Nazarewicz, B. K. Agrawal, N. Paar, and X. Roca-Maza, “Information content of the weak-charge form factor,” *Phys. Rev. C* **88**, 034325 (2013).
- [11] M. B. Tsang, J. R. Stone, F. Camera, P. Danielewicz, S. Gandolfi, K. Hebeler, C. J. Horowitz, Jenny Lee, W. G. Lynch, Z. Kohley, R. Lemmon, P. Möller, T. Murakami, S. Riordan, X. Roca-Maza, F. Sammarruca, A. W. Steiner, I. Vidaña, and S. J. Yennello, “Constraints on the symmetry energy and neutron skins from experiments and theory,” *Phys. Rev. C* **86**, 015803 (2012).
- [12] G. Hagen, A. Ekström, C. Forssén, G. R. Jansen, W. Nazarewicz, T. Papenbrock, K. A. Wendt, S. Bacca, N. Barnea, B. Carlsson, C. Drischler, K. Hebeler, M. Hjorth-Jensen, M. Miorelli, G. Orlandini, A. Schwenk, and J. Simonis, “Neutron and weak-charge distributions of the ^{48}Ca nucleus,” *Nature Physics* **12**, 186 (2016).
- [13] E. Epelbaum, H.-W. Hammer, and Ulf-G. Meißner, “Modern theory of nuclear forces,” *Rev. Mod. Phys.* **81**, 1773–1825 (2009).
- [14] R. Machleidt and D.R. Entem, “Chiral effective field theory and nuclear forces,” *Physics Reports* **503**, 1 – 75 (2011).
- [15] B. Alex Brown, “Neutron radii in nuclei and the neutron equation of state,” *Phys. Rev. Lett.* **85**, 5296–5299 (2000).
- [16] C. J. Horowitz and J. Piekarewicz, “Neutron star structure and the neutron radius of ^{208}pb ,” *Phys. Rev. Lett.* **86**, 5647–5650 (2001).
- [17] H. Kümmel, K. H. Lührmann, and J. G. Zabolitzky, “Many-fermion theory in expS- (or coupled cluster) form,” *Physics Reports* **36**, 1 – 63 (1978).
- [18] R. F. Bishop, “An overview of coupled cluster theory and its applications in physics,” *Theoretical Chemistry Accounts: Theory, Computation, and Modeling (Theoretica Chimica Acta)* **80**, 95–148 (1991).
- [19] Bogdan Mihaila and Jochen H. Heisenberg, “Microscopic Calculation of the Inclusive Electron Scattering Structure Function in ^{16}O ,” *Phys. Rev. Lett.* **84**, 1403–1406 (2000).
- [20] D. J. Dean and M. Hjorth-Jensen, “Coupled-cluster approach to nuclear physics,” *Phys. Rev. C* **69**, 054320 (2004).
- [21] Rodney J. Bartlett and Monika Musiał, “Coupled-cluster theory in quantum chemistry,” *Rev. Mod. Phys.* **79**, 291–352 (2007).
- [22] Sven Binder, Joachim Langhammer, Angelo Calci, and

- Robert Roth, “Ab initio path to heavy nuclei,” *Phys. Lett. B* **736**, 119 – 123 (2014).
- [23] G. Hagen, T. Papenbrock, M. Hjorth-Jensen, and D. J. Dean, “Coupled-cluster computations of atomic nuclei,” *Rep. Prog. Phys.* **77**, 096302 (2014).
- [24] W.H. Dickhoff and C. Barbieri, “Self-consistent green’s function method for nuclei and nuclear matter,” *Prog. Part. Nucl. Phys.* **52**, 377 – 496 (2004).
- [25] K. Tsukiyama, S. K. Bogner, and A. Schwenk, “In-Medium Similarity Renormalization Group For Nuclei,” *Phys. Rev. Lett.* **106**, 222502 (2011).
- [26] H. Hergert, S. K. Bogner, T. D. Morris, A. Schwenk, and K. Tsukiyama, “The in-medium similarity renormalization group: A novel ab initio method for nuclei,” *Phys. Rep.* **621**, 165 – 222 (2016).
- [27] V. Somà, C. Barbieri, and T. Duguet, “Ab initio gorkov-green’s function calculations of open-shell nuclei,” *Phys. Rev. C* **87**, 011303 (2013).
- [28] N. M. Parzuchowski, T. D. Morris, and S. K. Bogner, “Ab initio excited states from the in-medium similarity renormalization group,” *Phys. Rev. C* **95**, 044304 (2017).
- [29] N. M. Parzuchowski, S. R. Stroberg, P. Navrátil, H. Hergert, and S. K. Bogner, “Ab initio electromagnetic observables with the in-medium similarity renormalization group,” *Phys. Rev. C* **96**, 034324 (2017).
- [30] Carlo Barbieri, Francesco Raimondi, and Christopher McIlroy, “Recent Applications of Self-Consistent Green’s Function Theory to Nuclei,” in *12th International Spring Seminar on Nuclear Physics: Current Problems and Prospects for Nuclear Structure Sant’Angelo di Schia, Italy, May 15-19, 2017* (2017) arXiv:1711.04698 [nucl-th].
- [31] Petr Navrátil, Sofia Quaglioni, Ionel Stetcu, and Bruce R Barrett, “Recent developments in no-core shell-model calculations,” *Journal of Physics G: Nuclear and Particle Physics* **36**, 083101 (2009).
- [32] Evgeny Epelbaum, Hermann Krebs, Timo A. Lähde, Dean Lee, and Ulf-G. Meißner, “Structure and rotations of the hoyle state,” *Phys. Rev. Lett.* **109**, 252501 (2012).
- [33] Winfried Leidemann and Giuseppina Orlandini, “Modern Ab Initio Approaches and Applications in Few-Nucleon Physics with $A \geq 4$,” *Prog. Part. Nucl. Phys.* **68**, 158–214 (2013).
- [34] Bruce R. Barrett, Petr Navrátil, and James P. Vary, “Ab initio no core shell model,” *Prog. Part. Nucl. Phys.* **69**, 131 – 181 (2013).
- [35] J. Carlson, S. Gandolfi, F. Pederiva, Steven C. Pieper, R. Schiavilla, K. E. Schmidt, and R. B. Wiringa, “Quantum monte carlo methods for nuclear physics,” *Rev. Mod. Phys.* **87**, 1067–1118 (2015).
- [36] G. Hagen, G. R. Jansen, and T. Papenbrock, “Structure of ${}^{78}\text{Ni}$ from first-principles computations,” *Phys. Rev. Lett.* **117**, 172501 (2016).
- [37] J. Simonis, S. R. Stroberg, K. Hebeler, J. D. Holt, and A. Schwenk, “Saturation with chiral interactions and consequences for finite nuclei,” *Phys. Rev. C* **96**, 014303 (2017).
- [38] T. D. Morris, J. Simonis, S. R. Stroberg, C. Stumpf, G. Hagen, J. D. Holt, G. R. Jansen, T. Papenbrock, R. Roth, and A. Schwenk, “Structure of the lightest tin isotopes,” *Phys. Rev. Lett.* **120**, 152503 (2018).
- [39] G. Hagen, T. Papenbrock, D. J. Dean, and M. Hjorth-Jensen, “Medium-mass nuclei from chiral nucleon-nucleon interactions,” *Phys. Rev. Lett.* **101**, 092502 (2008).
- [40] G. Hagen, T. Papenbrock, D. J. Dean, and M. Hjorth-Jensen, “Ab initio coupled-cluster approach to nuclear structure with modern nucleon-nucleon interactions,” *Phys. Rev. C* **82**, 034330 (2010).
- [41] Robert Roth, Sven Binder, Klaus Vobig, Angelo Calci, Joachim Langhammer, and Petr Navrátil, “Medium-Mass Nuclei with Normal-Ordered Chiral $NN+3N$ Interactions,” *Phys. Rev. Lett.* **109**, 052501 (2012).
- [42] H. Hergert, S. K. Bogner, S. Binder, A. Calci, J. Langhammer, R. Roth, and A. Schwenk, “In-medium similarity renormalization group with chiral two- plus three-nucleon interactions,” *Phys. Rev. C* **87**, 034307 (2013).
- [43] V. Somà, A. Cipollone, C. Barbieri, P. Navrátil, and T. Duguet, “Chiral two- and three-nucleon forces along medium-mass isotope chains,” *Phys. Rev. C* **89**, 061301 (2014).
- [44] Sven Binder, Piotr Piecuch, Angelo Calci, Joachim Langhammer, Petr Navrátil, and Robert Roth, “Extension of coupled-cluster theory with a noniterative treatment of connected triply excited clusters to three-body hamiltonians,” *Phys. Rev. C* **88**, 054319 (2013).
- [45] Timo A. Lähde, Evgeny Epelbaum, Hermann Krebs, Dean Lee, Ulf-G. Meißner, and Gautam Rupak, “Lattice effective field theory for medium-mass nuclei,” *Phys. Lett. B* **732**, 110 – 115 (2014).
- [46] S. K. Bogner, T. T. S. Kuo, and A. Schwenk, “Model-independent low momentum nucleon interaction from phase shift equivalence,” *Physics Reports* **386**, 1 – 27 (2003).
- [47] S. K. Bogner, R. J. Furnstahl, and R. J. Perry, “Similarity renormalization group for nucleon-nucleon interactions,” *Phys. Rev. C* **75**, 061001 (2007).
- [48] A. Ekström, G. R. Jansen, K. A. Wendt, G. Hagen, T. Papenbrock, B. D. Carlsson, C. Forssén, M. Hjorth-Jensen, P. Navrátil, and W. Nazarewicz, “Accurate nuclear radii and binding energies from a chiral interaction,” *Phys. Rev. C* **91**, 051301 (2015).
- [49] S. Binder, A. Calci, E. Epelbaum, R. J. Furnstahl, J. Gollak, K. Hebeler, H. Kamada, H. Krebs, J. Langhammer, S. Liebig, P. Maris, Ulf-G. Meißner, D. Minossi, A. Nogga, H. Potter, R. Roth, R. Skibiński, K. Topolnicki, J. P. Vary, and H. Witała (LENPIC Collaboration), “Few-nucleon systems with state-of-the-art chiral nucleon-nucleon forces,” *Phys. Rev. C* **93**, 044002 (2016).
- [50] B. D. Carlsson, A. Ekström, C. Forssén, D. Fahlin Strömberg, G. R. Jansen, O. Lilja, M. Lindby, B. A. Mattsson, and K. A. Wendt, “Uncertainty analysis and order-by-order optimization of chiral nuclear interactions,” *Phys. Rev. X* **6**, 011019 (2016).
- [51] J. E. Lynn, I. Tews, J. Carlson, S. Gandolfi, A. Gezerlis, K. E. Schmidt, and A. Schwenk, “Chiral three-nucleon interactions in light nuclei, neutron- α scattering, and neutron matter,” *Phys. Rev. Lett.* **116**, 062501 (2016).
- [52] S. Bacca, M. A. Marchisio, N. Barnea, W. Leidemann, and G. Orlandini, “Microscopic calculation of six-body inelastic reactions with complete final state interaction: Photoabsorption of ${}^6\text{He}$ and ${}^6\text{Li}$,” *Phys. Rev. Lett.* **89**, 052502 (2002).
- [53] Doron Gazit, Sonia Bacca, Nir Barnea, Winfried Leidemann, and Giuseppina Orlandini, “Photoabsorption on ${}^4\text{He}$ with a realistic nuclear force,” *Phys. Rev. Lett.* **96**, 112301 (2006).

- [54] S. Bacca, H. Arenhövel, N. Barnea, W. Leidemann, and G. Orlandini, “Inclusive electron scattering off ${}^4\text{He}$,” *Phys. Rev. C* **76**, 014003 (2007).
- [55] V D Efron, W Leidemann, G Orlandini, and N Barnea, “The lorentz integral transform (lit) method and its applications to perturbation-induced reactions,” *Journal of Physics G: Nuclear and Particle Physics* **34**, R459 (2007).
- [56] S. Bacca and S. Pastore, “Electromagnetic reactions on light nuclei,” *Journal of Physics G: Nuclear and Particle Physics* **41**, 123002 (2014).
- [57] Victor D. Efron, Winfried Leidemann, and Giuseppina Orlandini, “Response functions from integral transforms with a lorentz kernel,” *Phys. Lett. B* **338**, 130 – 133 (1994).
- [58] S. Bacca, N. Barnea, G. Hagen, G. Orlandini, and T. Papenbrock, “First principles description of the giant dipole resonance in ${}^{16}\text{O}$,” *Phys. Rev. Lett.* **111**, 122502 (2013).
- [59] S. Bacca, N. Barnea, G. Hagen, M. Miorelli, G. Orlandini, and T. Papenbrock, “Giant and pigmy dipole resonances in ${}^4\text{He}$, ${}^{16,22}\text{O}$, and ${}^{40}\text{Ca}$ from chiral nucleon-nucleon interactions,” *Phys. Rev. C* **90**, 064619 (2014).
- [60] G. Hagen, M. Hjorth-Jensen, G. R. Jansen, and T. Papenbrock, “Emergent properties of nuclei from ab initio coupled-cluster calculations,” (2016), arXiv:1601.08203.
- [61] Angelo Calci, Petr Navrátil, Robert Roth, Jérémy Doherty, Sofia Quaglioni, and Guillaume Hupin, “Can Ab Initio Theory Explain the Phenomenon of Parity Inversion in ${}^{11}\text{Be}$?” *Phys. Rev. Lett.* **117**, 242501 (2016), arXiv:1608.03318 [nucl-th].
- [62] A. Lovato, S. Gandolfi, J. Carlson, Steven C. Pieper, and R. Schiavilla, “Electromagnetic response of ${}^{12}\text{C}$: A first-principles calculation,” *Phys. Rev. Lett.* **117**, 082501 (2016), arXiv:1605.00248 [nucl-th].
- [63] Christina Stumpf, Tobias Wolfgruber, and Robert Roth, “Electromagnetic Strength Distributions from the Ab Initio No-Core Shell Model,” (2017), arXiv:1709.06840 [nucl-th].
- [64] N. Rocco and C. Barbieri, “Inclusive electron-nucleus cross section within the Self Consistent Green’s Function approach,” (2018), arXiv:1803.00825 [nucl-th].
- [65] D. R. Entem and R. Machleidt, “Accurate charge-dependent nucleon-nucleon potential at fourth order of chiral perturbation theory,” *Phys. Rev. C* **68**, 041001 (2003).
- [66] A. Ekström, B. D. Carlsson, K. A. Wendt, C. Forssén, M. Hjorth Jensen, R. Machleidt, and S. M. Wild, “Statistical uncertainties of a chiral interaction at next-to-next-to leading order,” *J. Phys. G* **42**, 034003 (2015).
- [67] R. Navarro Pérez, J. E. Amaro, and E. Ruiz Arriola, “Low-energy chiral two-pion exchange potential with statistical uncertainties,” *Phys. Rev. C* **91**, 054002 (2015).
- [68] K. Hebeler, S. K. Bogner, R. J. Furnstahl, A. Nogga, and A. Schwenk, “Improved nuclear matter calculations from chiral low-momentum interactions,” *Phys. Rev. C* **83**, 031301 (2011).
- [69] Angelo Calci and Robert Roth, “Sensitivities and correlations of nuclear structure observables emerging from chiral interactions,” *Phys. Rev. C* **94**, 014322 (2016).
- [70] J. S. Levinger and H. A. Bethe, “Dipole transitions in the nuclear photo-effect,” *Phys. Rev.* **78**, 115–129 (1950).
- [71] D.M. Brink, “Individual particle and collective aspects of the nuclear photoeffect,” *Nuclear Physics* **4**, 215 – 220 (1957).
- [72] L. L. Foldy, “Photodisintegration of the lightest nuclei,” *Phys. Rev.* **107**, 1303–1305 (1957).
- [73] A. Dellafiore and E. Lipparini, “Bremsstrahlung sum rule and nuclear charge distribution,” *Nuclear Physics A* **388**, 639 – 643 (1982).
- [74] J.L Friar, “Low-energy theorems for nuclear compton and raman scattering and $0+ \rightarrow 0+$ two-photon decays in nuclei,” *Annals of Physics* **95**, 170 – 201 (1975).
- [75] F. Coester, “Bound states of a many-particle system,” *Nuclear Physics* **7**, 421 – 424 (1958).
- [76] F. Coester and H. Kümmel, “Short-range correlations in nuclear wave functions,” *Nuclear Physics* **17**, 477 – 485 (1960).
- [77] M. Wloch, D. J. Dean, J. R. Gour, M. Hjorth-Jensen, K. Kowalski, T. Papenbrock, and P. Piecuch, “*Ab-Initio* coupled-cluster study of ${}^{16}\text{O}$,” *Phys. Rev. Lett.* **94**, 212501 (2005).
- [78] John F. Stanton and Rodney J. Bartlett, “The equation of motion coupledcluster method. a systematic biorthogonal approach to molecular excitation energies, transition probabilities, and excited state properties,” *J. Chem. Phys.* **98**, 7029–7039 (1993).
- [79] M. Miorelli, S. Bacca, N. Barnea, G. Hagen, G. R. Jansen, G. Orlandini, and T. Papenbrock, “Electric dipole polarizability from first principles calculations,” ArXiv e-prints (2016), arXiv:1604.05381 [nucl-th].
- [80] Yoon S. Lee, Stanislaw A. Kucharski, and Rodney J. Bartlett, “A coupled cluster approach with triple excitations,” *The Journal of Chemical Physics* **81**, 5906–5912 (1984).
- [81] I. Shavitt and R. J. Bartlett, *Many-body Methods in Chemistry and Physics* (Cambridge University Press, Cambridge UK, 2009).
- [82] J. D. Watts and R. J. Bartlett, “Economical triple excitation equation-of-motion coupled-cluster methods for excitation energies,” *Chem. Phys. Lett.* **233**, 81 – 87 (1995).
- [83] G. R. Jansen, M. D. Schuster, A. Signoracci, G. Hagen, and P. Navrátil, “Open *sd*-shell nuclei from first principles,” *Phys. Rev. C* **94**, 011301 (2016).
- [84] M. Miorelli, *Electromagnetic processes of medium-mass nuclei from coupled-cluster theory*, Ph.D. thesis, The University of British Columbia (2017).
- [85] Nir Barnea, Winfried Leidemann, and Giuseppina Orlandini, “State-dependent effective interaction for the hyperspherical formalism with noncentral forces,” *Nuclear Physics A* **693**, 565 – 578 (2001).
- [86] J. Ahrens, H. Borchert, K.H. Czock, H.B. Eppler, H. Gimm, H. Gundrum, M. Kröning, P. Riehn, G. Sita Ram, A. Zieger, and B. Ziegler, “Total nuclear photon absorption cross sections for some light elements,” *Nucl. Phys. A* **251**, 479 – 492 (1975).
- [87] Andreas Nogga, Scott K. Bogner, and Achim Schwenk, “Low-momentum interaction in few-nucleon systems,” *Phys. Rev. C* **70**, 061002 (2004).